Redox Biology 52 (2022) 102288

Contents lists available at ScienceDirect

Redox Biology

journal homepage: www.elsevier.com/locate/redox

# Empagliflozin attenuates cardiac microvascular ischemia/reperfusion through activating the AMPKα1/ULK1/FUNDC1/mitophagy pathway

Chen Cai [a,1], Zhongzhou Guo [b,1], Xing Chang [c,1], Ziying Li [a,1], Feng Wu [a], Jing He [a], Tiantian Cao [a], Kangrong Wang [a], Nengxian Shi [a], Hao Zhou [d], Sam Toan [e], David Muid [f], Ying Tan [a,*]

[a] Department of Critical Care Medicine, Nanfang Hospital, Southern Medical University/The First School of Clinical Medicine, Southern Medical University, Guangzhou, 510515, China
[b] Department of Pharmacy, Zhujiang Hospital, Southern Medical University, Guangzhou, 510280, China
[c] Guang'anmen Hospital, China Academy of Chinese Medical Sciences, Beijing, 100053, China
[d] Center for Cardiovascular Research and Alternative Medicine, University of Wyoming College of Health Sciences, Laramie, WYWY, 82071, USA
[e] Department of Chemical Engineering, University of Minnesota-Duluth, Duluth, MN, 55812, USA
[f] Perelman School of Medicine, University of Pennsylvania, Philadelphia, PA, USA

ARTICLE INFO

*Keywords:*
Empagliflozin
Cardiac microvascular I/R injury
AMPKα1/ULK1 pathway
FUNDC1-Dependent mitophagy

ABSTRACT

Mitophagy preserves microvascular structure and function during myocardial ischemia/reperfusion (I/R) injury. Empagliflozin, an anti-diabetes drug, may also protect mitochondria. We explored whether empagliflozin could reduce cardiac microvascular I/R injury by enhancing mitophagy. In mice, I/R injury induced luminal stenosis, microvessel wall damage, erythrocyte accumulation and perfusion defects in the myocardial microcirculation. Additionally, I/R triggered endothelial hyperpermeability and myocardial neutrophil infiltration, which upregulated adhesive factors and endothelin-1 but downregulated vascular endothelial cadherin and endothelial nitric oxide synthase in heart tissue. *In vitro*, I/R impaired the endothelial barrier function and integrity of cardiac microvascular endothelial cells (CMECs), while empagliflozin preserved CMEC homeostasis and thus maintained cardiac microvascular structure and function. I/R activated mitochondrial fission, oxidative stress and apoptotic signaling in CMECs, whereas empagliflozin normalized mitochondrial fission and fusion, neutralized supraphysiologic reactive oxygen species concentrations and suppressed mitochondrial apoptosis. Empagliflozin exerted these protective effects by activating FUNDC1-dependent mitophagy through the AMPKα1/ULK1 pathway. Both *in vitro* and *in vivo,* genetic ablation of *AMPKα1* or *FUNDC1* abolished the beneficial effects of empagliflozin on the myocardial microvasculature and CMECs. Taken together, the preservation of mitochondrial function through an activation of the AMPKα1/ULK1/FUNDC1/mitophagy pathway is the working mechanism of empagliflozin in attenuating cardiac microvascular I/R injury.

## 1. Introduction

Coronary thrombosis can induce ischemic stress in the heart by restricting the flow of fresh oxygen and nutrients to the myocardium, thus triggering oxidative stress, calcium overload and apoptosis in cardiomyocytes [1]. The pathological course of myocardial ischemia is often termed as myocardial infarction, which has been ranked as the main cause of death in elderly patients. The standard therapeutic approach for myocardial infarction is the rapid and timely restoration of the coronary blood flow to the ischemic heart. Although such reperfusion strategies can alleviate ischemic damage, the re-introduction of fresh blood is always associated with additional damage to the post-ischemic myocardium [2]. The occurrence of ischemia/reperfusion (I/R) injury increases the morbidity and mortality of myocardial infarction, thus limiting the clinical benefits of reperfusion strategies [3]. Compared to cardiomyocyte I/R injury, cardiac microvascular I/R injury is a neglected topic [4,5], so its molecular mechanism is not fully understood and few drugs have been validated or used for its

* Corresponding author.
*E-mail address:* tanying0924@163.com (Y. Tan).
[1] These authors contributed to this article equally.

https://doi.org/10.1016/j.redox.2022.102288
Received 7 February 2022; Received in revised form 7 March 2022; Accepted 12 March 2022
Available online 18 March 2022

management.

Mitochondria are crucial for coordinating extracellular damage signals and maintaining cardiac microvascular endothelial function [6]. When myocardial perfusion is restricted, energy metabolism in cardiac microvascular endothelial cells is reduced; thus, mitochondrial fission is activated to augment the mitochondrial population and meet the cellular metabolic demand [7]. However, pathological mitochondrial fission damages mitochondrial DNA (mtDNA) during mitosis, thus impairing mitochondrial redox biology, triggering oxidative stress, reducing the mitochondrial membrane potential and inducing the opening of the mitochondrial permeability transition pore (mPTP) [7,8]. Under such conditions, mitochondria switch from electric generators to endothelial apoptosis inducers [9]. Endothelial cell dysfunction or death contributes to microvessel swelling and vascular wall collapse, further interrupting the flow of fresh blood to the post-ischemic myocardium [10,11].

Mitophagy is the evolutionarily conserved process of repairing poorly structured mitochondria with the help of lysosomes [11]. Mitophagy has been reported to preserve microvascular structure and function under various pathophysiological conditions, including myocardial I/R injury [4], diabetes-related microvascular damage [12], sepsis-associated microcirculatory injury [13] and smoke-induced pulmonary endothelial injury [14]. However, it has been difficult to find an effective drug that specifically activates mitophagy and alleviates mitochondrial damage to improve the resistance of microvessels to I/R injury.

Empagliflozin is a novel anti-diabetes drug that promotes the urinary excretion of glucose [15]. In the EMPA-REG OUTCOME clinical trial [16], empagliflozin treatment was found to reduce the risk of death from cardiovascular causes in diabetic patients with cardiovascular disease. Functional analyses indicated that empagliflozin administration improved the ratio of adenosine monophosphate (AMP) to adenosine triphosphate (ATP) in cardiomyocytes, thus accelerating glucose metabolism and increasing cell viability [17]. Animal studies and molecular experiments have illustrated that empagliflozin protects not only cardiomyocytes, but also endothelial cells; for instance, empagliflozin increased phosphorylated endothelial nitric oxide synthase (p-eNOS) expression and nitric oxide production in cardiac endothelial cells in a murine model of heart failure [18]. Empagliflozin also attenuated oxidative stress-induced endothelial barrier dysfunction through an undefined mechanism [19]. Regarding mitochondrial biology, empagliflozin was found to inhibit hyperglycemia-induced mitochondrial fission [20] and lipopolysaccharide-stimulated mitochondrial oxidative stress [21] by activating AMP-activated protein kinase catalytic subunit alpha 1 (AMPKα1).

Based on the above data, we investigated whether empagliflozin could protect against cardiac microvascular I/R injury by sustaining mitochondrial homeostasis. We specifically examined whether empagliflozin could ameliorate I/R-induced endothelial mitochondrial damage by activating mitophagy, and assessed its molecular mechanism in cardiac microvascular I/R injury.

## 2. Materials and methods

### 2.1. Mice

AMPKα1$^{f/f}$ mutant mice (stock no.: 014141, The Jackson Laboratory) possess loxP sites flanking exon 3 of the *Prkaa1* gene. FUNDC1$^{f/f}$ mutant mice were generated as our previously described [22]. Tie2$^{Cre}$ (Tek-Cre) transgenic mice have the mouse endothelial-specific receptor tyrosine kinase (Tek or Tie2) promoter directing the expression of Cre recombinase (stock no.: 008863, The Jackson Laboratory). Either AMPKα1$^{f/f}$ mutant mice or FUNDC1$^{f/f}$ mutant mice were crossed with Tie2$^{Cre}$ mice to generate endothelial-specific *AMPKα1*-knockout (AMPKα1$^{EKO}$) mice or endothelial-specific *FUNDC1*-knockout (FUNDC1$^{EKO}$) mice. Tie2$^{Cre}$ mice served as controls. All mice were maintained on a C57BL/6 background and were used in this study at the age of 10 weeks. Male mice were used, as they are the best-validated model for cardiac I/R injury, and male gender is well recognized as a significant risk factor for cardiovascular diseases.

### 2.2. Mouse model of myocardial I/R injury

All experiments were conducted according to the ethical committee guidelines for animal experimentation of Southern Medical University. The mice were randomly assigned to either the sham operation group or the myocardial ischemia (45 min)/reperfusion (2 h) (I/R) injury group. A single sequence of simple random assignments was used, in accordance with previous studies [23]. Allocation concealment was established using ear tag-based sequentially numbered mice. Mice (10 weeks old) were treated with empagliflozin (10 mg/kg/d) seven days before myocardial I/R injury, in accordance with a previous study [20,24]. Empagliflozin was kindly provided by Boehringer Ingelheim Pharma GmbH & Co. KG, Germany, and was administered via oral gavage with 0.5% hydroxyethylcellulose as the vehicle. Compound C (CC, Selleck, Cat. S7306, 10 mg/kg/d) was used to inhibit empagliflozin-induced AMPK activation in certain mice (the CC group).

### 2.3. Echocardiography

Two-dimensional echocardiography was performed in anesthetized mice (3.0% isoflurane with $O_2$ flow at 1.0 L/min) using Vevo 2100 echo with the MS400 transducer. Echocardiographic images were recorded along parasternal short axis, and then analyzed off-line (Vevo 2100 software) by an observer blinded to the treatment groups. Ejection fractions (%EF) and percent fractional shortening (%FS) were calculated [25].

### 2.4. CMEC isolation

CMECs were isolated from mice after myocardial I/R injury, in accordance with previous research [26,27]. In brief, isolated hearts were washed extensively with Hanks' Balanced Salt Solution with $Ca^{2+}$ and $Mg^{2+}$ in a Petri dish. The atria and right ventricle were removed, while the left ventricle was used for subsequent experiments. Excised pieces of the left ventricle were incubated with 0.2% (w/v) collagenase type I (Gibco, USA) for 10 min and 0.25% (w/v) trypsin (Hyclone, USA) for 5 min at 37 °C in a shaking bath. After the final dissociation step, collagenase was neutralized through the addition of 500 μL of fetal bovine serum, and the mixture was transferred through a filter (200 μM) into a 50-mL Falcon tube. The filtrates were centrifuged at 80×*g* at 4 °C for 1 min. The sedimented CMECs at the bottom of the tube were resuspended in 5 mL of Hanks' Balanced Salt Solution I plus bovine serum albumin, and were plated in a 6-cm$^2$ dish at 37 °C [28].

### 2.5. Transmission electron microscopy

Heart tissues were fixed with 2.5% glutaraldehyde, 2.5% polyvidone 25 and 0.1 M sodium cacodylate (pH 7.4). After being washed with 0.1 M sodium cacodylate buffer (pH 7.4), the samples were post-fixed in the same buffer containing 2% osmium tetroxide and 1.5% potassium ferrocyanide for 1 h [8]. The samples were then washed in water, contrasted en bloc with uranyl acetate, dehydrated using an ascending ethanol series and embedded in a Durcupan ACM-based resin [29]. Ultrathin sections were cut with a Reichert Ultracut S ultramicrotome (Science Service, Munich, Germany) and contrasted with lead citrate. Images were viewed and captured with an EM 10 CR electron microscope (Carl Zeiss Gemini, Germany), and were analyzed by an independent blinded investigator [30].

### 2.6. qRT-PCR

All reagents and containers used for RNA processing were RNase-free grade or treated with 0.1% DEPC (4387937, Thermo Fisher) to eliminate RNase contaminants. Total RNA was extracted in TRIzol (15596018, Invitrogen) according to the manufacturer's instructions [7]. Reverse transcription of 500 ng RNA was performed to synthesize cDNA using random primers (SO142, Thermo Fisher) and RevertAid H Minus Reverse Transcriptase (EP0452, Thermo Fisher) according to the manufacturer's instructions [31]. The qPCR assays were carried out on a StepOnePlus system (Applied Biosystem) using SYBR Green Master Kit (A25918, Thermo Fisher). Three biological replicates per condition were measured. Gene expression was normalized to *GAPDH* expression, and changes in gene expression were calculated using the $2^{-\Delta\Delta CT}$ method. The primers used in our study were as follows: TNFα (Forward, 5′-AGATGGAGCAACCTAAGGTC-3'; Reverse, 5′GCAGACCTCGCTGTTCTAGC-3′), IL6 (Forward, 5′-CAGACTCGCGCCTCTAAGGAGT3'; Reverse, 5′-GATAGCCGATCCGTCGAA-3′), MCP1 (Forward, 5′GGATGGATTGCACAGCCATT-3'; Reverse, 5′-GCGCCGACTCAGAGGTGT-3′).

### 2.7. Western blotting

Tissues and cells were lysed in RIPA buffer (R0278, Sigma-Aldrich) supplemented with protease inhibitors (36978, Thermo Fisher) and phosphatase inhibitors (P5726, Sigma-Aldrich) on ice for 10 min. The lysates were collected and centrifuged at 14000 rpm for 15 min at 4 °C. Total protein concentrations in the supernatant were determined by a Bio-Rad protein assay kit (5000113–115, Bio Rad, Bradford method). Following the addition of LDS sample buffer (4x, NP0007, Life-technologies) [32], the samples were boiled at 90 °C for 10 min. Twenty microgram proteins were separated by 10–15% SDS-PAGE and transferred onto 0.2 μm nitrocellulose membranes (4685.1, Carl Roth). Following blocking with 5% non-fat milk for 1 h at room temperature, the membranes were incubated with primary antibodies at 4 °C overnight. The next day, the membranes were incubated with secondary antibodies for 1 h. After washing by Tris buffered saline with 0.05% Tween 20 (TBST) three times, the membranes were incubated visualized by the Pierce™ ECL Plus Western Blotting Substrate (32132, Life-technologies) using the ChemiDoc gel imaging system (BIORAD). Intensity of each protein strips was quantified using Image J software. Primary antibodies for immunoblotting were as follows: ET-1 (1:1000, Abcam, #ab178454), eNOS (1:1000, Abcam, #ab199956), p-eNOS (1:1000, Abcam, #ab215717), Fak (1:1000, Abcam, #ab40794), Src (1:1000, Abcam, #ab133283), Fak (1:1000, Abcam, #ab40794), Drp1 (1:1000, Abcam, #ab184247), p-Drp1 (1:1000, Cell Signaling Technology, #4494), FUNDC1 (1:1000, Abcam, #ab224722), Fis1 (1:1000, Abcam, #ab156865), Mfn2 (1:1000, Abcam, #ab124773), Opa1 (1:1000, Abcam, #ab227868), GAPDH (1:1000, Abcam, #ab8245), Atg5 (1:1000, Abcam, #ab108327), Beclin1 (1:1000, Abcam, #ab207612), p62 (1:1000, Abcam, #ab91526), LC3II (1:1000, Abcam, #ab192890), Tom20 (1:1000, Abcam, #ab186735), AMPK (1:1000, Abcam, #ab186735), p-AMPK (1:1000, Abcam, #ab131357), ULK1 (1:1000, Abcam, #ab167139), p-ULK1 (1:1000, Abcam, #ab229909).

### 2.8. Histological analysis

Heart tissues were fixed in 4% paraformaldehyde and embedded in paraffin using standard procedures [33]. After deparaffinization and rehydration of the tissue sections, H&E staining was performed to assess the erythrocyte morphology. Images were acquired with a light microscope (Olympus, Japan). Immunohistochemistry was performed as previously described [11].

### 2.9. Immunofluorescence

For immunofluorescence analyses of colocalization, cells were fixed for 30 min at room temperature with 4% paraformaldehyde, and then were permeabilized with 0.2% Triton X-100. Subsequently, the cells were incubated in a blocking solution of phosphate-buffered saline/Tween-20 with 10% goat serum and 3% bovine serum albumin for 1 h at room temperature [34]. The samples were then incubated with the primary antibodies overnight at 4 °C, and with appropriate fluorescent secondary antibodies for 3 h at room temperature. The nuclei were stained with 4',6-diamidino-2-phenylindole (DAPI). Images were captured with a laser-scanning confocal microscope (LSM700; Carl Zeiss Inc., Oberkochen, Germany). Primary antibodies for immunoblotting were as follows: Gr1 (1:500, Abcam, #ab25377), troponin T (1:500, Abcam, #ab8295), CD31 (1:500, Abcam, #ab222783), VE-Cadherin (1:500, Abcam, #ab33168), Tom-20 (1:500, Abcam, # ab78547). Mitophagy was determined through mt-Kemia as our previously described [22].

### 2.10. siRNA transfection

Confluent cells were seeded 24 h before transfection. AMPK small interfering RNAs (siRNA-AMPK) were transfected into cells using Lipofectamine RNAiMAX reagent (13778–075, Thermo Fisher) according to the manufacturer's instruction [35]. The transfected cells were incubated at 37 °C for 48 h, followed by extraction of cellular DNA, RNA and proteins. A non-targeting negative stealth siRNA (scrambled, sc-37007, Santa Cruz) was used as a negative control [36].

### 2.11. ROS staining, mitochondrial membrane potential measurement and mPTP opening detection

Mitochondrial and cytoplasmic ROS levels were measured in CMECs plated on six-well dishes at equal densities [37]. For ROS measurements, the cells were washed with phosphate-buffered saline and then stained with the mitochondrial ROS indicator MitoSOX™ Red (2 μmol/L, M36008; Invitrogen) and the cytoplasmic ROS probe CM-H2DCFDA (C6827; Invitrogen) at 37 °C for 15 min. The mitochondrial membrane potential was detected using the JC-1 probe according to the manufacturer's instructions (T3168; Invitrogen). Cell images were obtained using a confocal fluorescence microscope (LSM 880 with AiryScan) and ZEN BLUE imaging software. The opening of the mPTP was visualized based on the rapid dissipation of tetramethylrhodamine ethyl ester (TMRE) fluorescence, as reported previously [7].

### 2.12. ImageJ quantitative analysis

Confocal micrographs of CMEC confocal fluorescence images were analyzed using the ImageJ fluorescence measuring function (NIH Image, Bethesda, MD, USA). The relative fluorescence intensity was determined using randomly selected cross-sections of CMECs. The fluorescent intensities were extracted, and individual images were normalized to the average background intensity [38]. During quantitation, RGB images were converted to 32-bit grayscale images. The grayscale images were adjusted for brightness and contrast to exclude noise pixels. The threshold was also adjusted to highlight all positive pixels (green or red fluorescence) to be measured [39]. The background fluorescence intensity was measured using five different areas of the images. The staining intensity was then calculated as the integrated density minus the background intensity. The values (expressed as Area %) from each measurement were averaged and expressed as the mean ± standard error [40].

### 2.13. Enzyme-linked immunosorbent assay (ELISA)

The activity levels of intracellular anti-oxidative molecules were determined using commercially available ELISA kits (GSH: cat. no. EIAGSHC, Invitrogen; SOD: cat. no. EIASODC, Invitrogen; GPX: cat. no. MBS776262, MyBioSource, USA) according to the manufacturers'

instructions. Caspase-9 activity (Mouse Caspase-9 ELISA kit, cat. no. MBS458138, MyBioSource) and ATP production (ATP/Adenosine Triphosphate ELISA kit, cat. no. LS-F24998, LifeSpan BioSciences, USA) were determined based on the manufacturers' instructions. After the addition of the stop solution, the absorbance was measured at 450 nm (ELx800, BioTek Instruments) [41].

### 2.14. Statistics

All values are expressed as the mean ± standard error. The sample numbers are provided in the individual Figure legends and represent biological replicates. All raw data and results were interpreted in a blinded fashion. The representative image for each group was selected based on the mean value after quantitative analysis. Statistical analyses were performed with GraphPad Prism software (version 7.01). For comparisons of two groups, Student's t-test was used. For comparisons of more than two groups, one-way or two-way analysis of variance was used, with Bonferroni's or Dunnett's multiple-comparisons test for normally distributed data or the Mann-Whitney test for non-normally distributed data. Unless otherwise stated, $p < 0.05$ was considered statistically significant.

## 3. Results

### 3.1. Empagliflozin reduces I/R-induced microvascular damage

In this study, mice were subjected to myocardial I/R injury or a sham operation, with or without prior treatment with empagliflozin. To determine the effects of empagliflozin on cardiac microvascular damage, we used an electron microscope to examine the microvascular structure of the reperfused heart. As shown in Fig. 1A, microvascular endothelial cell inflation and luminal stenosis were observed in I/R-treated mice compared with sham-operated control mice. Empagliflozin inhibited these changes in the microvascular ultrastructure, as evidenced by the smooth endothelial cells and regular vascular walls in the drug-treated group.

Microvascular structural impairments will slow the blood flow or even induce the occlusion of the microcirculation. Reduced blood perfusion can change the local fluid mechanics from laminar to turbulent blood flow, thus promoting erythrocyte accumulation and thrombosis. Hematoxylin and eosin (H&E) staining of heart tissue revealed that erythrocytes gathered into a mass after I/R injury (Fig. 1B). Interestingly, empagliflozin treatment sustained the linear morphology of erythrocytes and prevented their convergence in microvessels, suggesting that empagliflozin reduced the risk of microthrombus formation during I/R injury. In addition to a reduced blood flow and microvascular obstruction, microvascular I/R injury is associated with microcirculatory hyperpermeability, which leads to myocardial inflammatory responses and swelling. Immunofluorescence staining revealed that $Gr1^+$ neutrophil levels in the myocardium were elevated after I/R injury (Fig. 1C and D), and quantitative real-time PCR (qRT-PCR) revealed that inflammatory cytokines such as tumor necrosis factor α (*TNFα*), monocyte chemotactic protein 1 (*MCP1*) and interleukin 6 (*IL-6*) were upregulated (Fig. 1E–G). Empagliflozin prevented the permeation of $Gr1^+$ neutrophils into the myocardium and therefore suppressed the transcription of these inflammatory cytokines. These data indicated that empagliflozin ameliorated I/R-induced microvascular ultrastructural damage by maintaining normal local fluid mechanics and preventing luminal obstruction, microvessel hyperpermeability and myocardial inflammatory responses.

### 3.2. Empagliflozin suppresses I/R-induced endothelial cell damage

The cardiac microcirculation is composed of a monolayer of endothelial cells, which are known as cardiac microvascular endothelial cells (CMECs). Ample studies have identified CMEC dysfunction or death as a pathological feature of cardiac microvascular I/R injury [42,43]; thus, we assessed the effects of empagliflozin on endothelial cells. CMECs synthesize and release nitric oxide via eNOS, thereby promoting vascular relaxation. We found that p-eNOS was downregulated in heart tissue following I/R injury, whereas the endothelial vasoconstrictor endothelin-1 (ET-1) was rapidly upregulated (Fig. 2A–C). Empagliflozin supplementation restored the cellular levels of p-eNOS while repressing ET-1 expression in the reperfused heart (Fig. 2A–C).

Reduced eNOS activity has been associated with endothelial dysfunction, which is characterized by impaired endothelial integrity and barrier function. Immunofluorescence analyses of endothelial integrity revealed that endothelial junctional proteins such as vascular endothelial (VE)-cadherin were slightly downregulated in the I/R injury group compared with the sham group (Fig. 2D and E). In contrast,

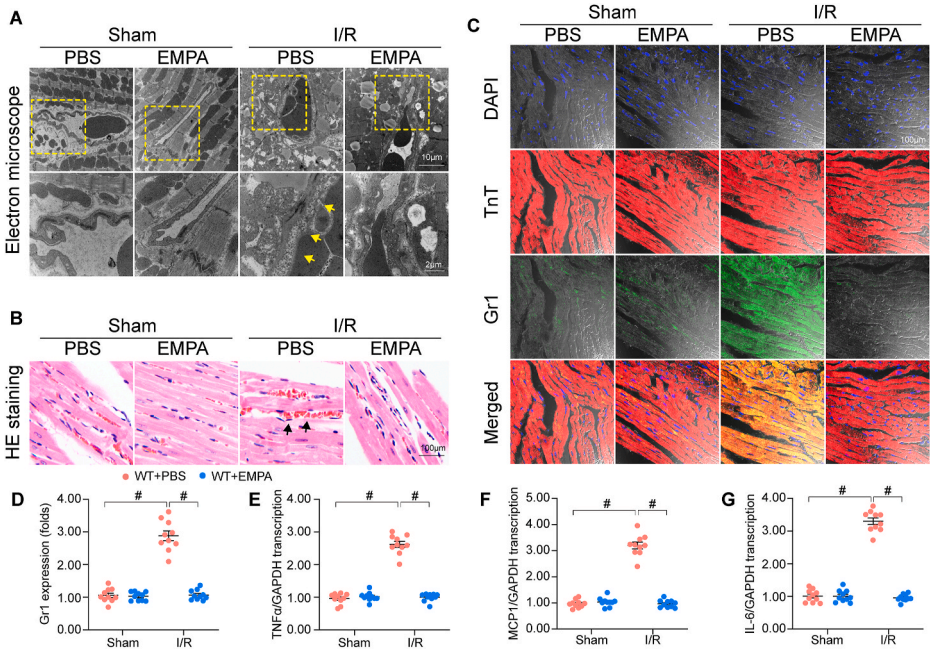


**Fig. 1. Empagliflozin attenuates I/R-induced cardiac microvascular damage.** Mice were assigned to the sham operation group or the myocardial I/R injury group. Empagliflozin (10 mg/kg/d) was administered seven days before myocardial I/R injury. **(A)** An electron microscope was used to detect changes in the microvascular structure of the reperfused heart. Yellow arrows indicate microvascular endothelial cell inflation and luminal stenosis. **(B)** Heart tissue was stained using H&E to visualize the morphology of erythrocytes. Black arrows indicate erythrocyte accumulation in microvessels. **(C–D)** Double immunofluorescence staining of $Gr1^+$ neutrophils and troponin T $(TnT)^+$ cardiomyocytes. DAPI was used to visualize the nucleus in the myocardium. **(E–G)** RNA was isolated from heart tissues, and qRT-PCR was used to determine the expression of inflammatory cytokines (*TNFα*, *MCP1* and *IL-6*). Experiments were repeated at least three times and the data are shown as mean ± SEM (n = 6 mice or three independent cell isolations per group). *$p < 0.05$. (For interpretation of the references to colour in this figure legend, the reader is referred to the Web version of this article.)

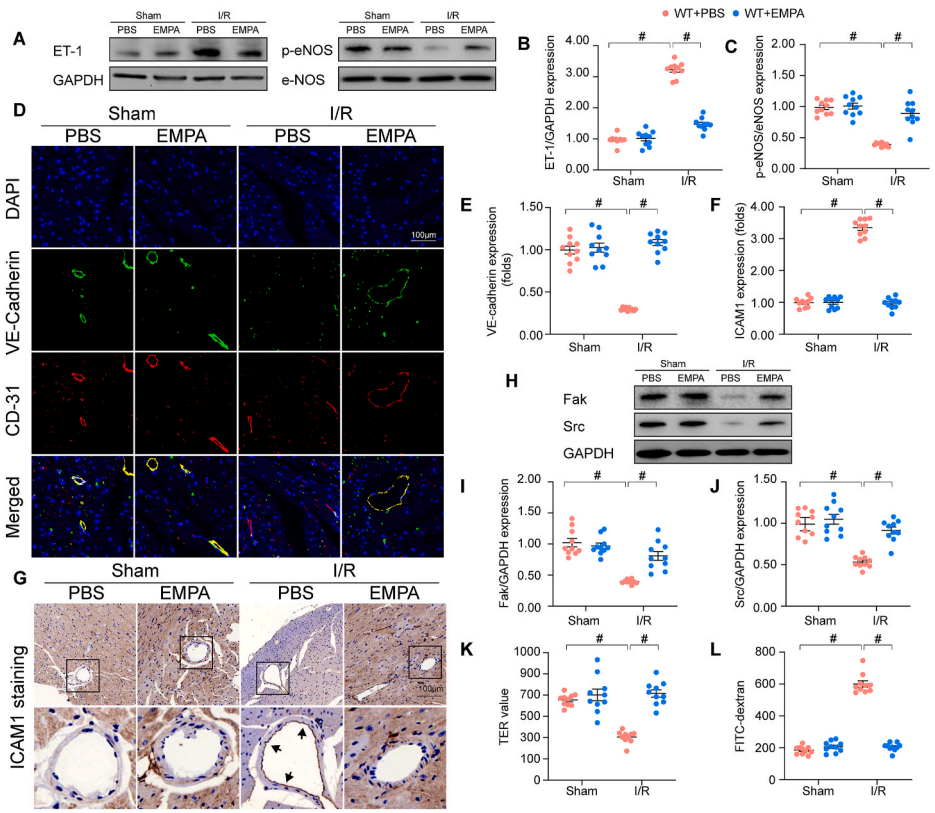


**Fig. 2. Empagliflozin alleviates I/R-induced CMEC damage.** *In vivo*, mice were assigned to the sham operation group or the myocardial I/R injury group. Empagliflozin (10 mg/kg/d) was administered seven days before myocardial I/R injury. *In vitro*, CMECs were isolated from I/R- or empagliflozin-treated hearts. The cells were cultured for 24 h and then used for functional analyses. **(A–C)** *In vivo*, proteins were isolated from reperfused heart tissues, and Western blots were used to analyze eNOS and ET-1 levels. **(D, E)** *In vivo*, immunofluorescence staining of VE-cadherin was performed to observe the changes in endothelial integrity and barrier function. **(F, G)** Immunohistochemistry was used to assess the expression of ICAM1, an endothelium-specific adhesive factor. **(H–J)** Proteins were isolated from CMECs, and the levels of Src and Fak were analyzed through Western blots. **(K, L)** *In vitro*, FITC-dextran clearance and TER assays were used to analyze the endothelial barrier function and integrity of CMECs. Experiments were repeated at least three times and the data are shown as mean ± SEM (n = 6 mice or three independent cell isolations per group). *p < 0.05.

intercellular adhesion molecule 1 (ICAM1, an adhesive factor) was upregulated in CMECs after I/R injury (Fig. 2F and G). Empagliflozin restored VE-cadherin expression and inhibited ICAM1 expression in CMECs after I/R injury. At the molecular level, VE-cadherin activity is mainly regulated by Src and focal adhesion kinase (Fak). In CMECs, Src and Fak levels were significantly reduced following I/R injury, but returned to normal following empagliflozin treatment (Fig. 2H–J).

To further assess endothelial barrier function and integrity, we isolated CMECs from sham-operated or I/R-treated mice. Then, we performed fluorescein isothiocyanate (FITC)-dextran clearance and transendothelial electrical resistance (TER) assays. As shown in Fig. 2K and L, I/R injury elevated the remaining FITC-dextran content and reduced the TER value compared with the control group, reflecting an impaired CMEC adhesion capacity. However, empagliflozin treatment prevented FITC-dextran accumulation and increased the TER value. These data suggested that empagliflozin maintained CMEC function and integrity in the setting of cardiac I/R injury.

To understand whether the improvements in microvascular structure and endothelial function are associated with increased cardiac function, echocardiography was used to analyze the alterations of myocardial performance. The data shown in Table 1 demonstrated that the reduction of ejection fraction and the dilation of left ventricular dimension in the empagliflozin group were not as remarkable as those of the I/R group. These results highlight that empagliflozin-mediated microvascular protection may improve cardiac function during I/R injury.

### 3.3. *Empagliflozin alleviates I/R-induced endothelial mitochondrial dysfunction*

Mitochondrial damage has been reported to contribute to I/R-induced endothelial damage. We performed Western blot analyses, which demonstrated that I/R injury activated mitochondrial fission but inhibited mitochondrial fusion in CMECs (Fig. 3A–E). To confirm these findings, we subjected CMECs to immunofluorescence analyses, which

**Table 1**
**The difference of echocardiography parameter and cardiac/body weight between mice treated with empagliflozin (EMPA) after ischemia/reperfusion injury.** BW, body weight; HW, heart weight; LVDd, diastolic dimension of left ventricle; LVDs, systolic dimension of left ventricle; IVS, thickness of interventricular septum; PW, thickness of posterior wall; PW, thickness of posterior wall; FS, ratio of left ventricular fractional shortening; HR, heart rate; bmp, beats/min; #p < 0.05 vs. sham, *p < 0.05 vs. I/R.

| Parameter | Sham + PBS | Sham + EMPA | I/R + PBS | I/R + EMPA |
|---|---|---|---|---|
| BW, g | 26.0 ± 1.0 | 26.1 ± 0.8 | 25.9 ± 0.7 | 25.9 ± 0.9 |
| HW, mg | 156.4 ± 7.8 | 154.2 ± 8.3 | 237.6 ± 1.2# | 186.4 ± 9.6* |
| HW/BW, mg/g | 6.04 ± 0.33 | 5.94 ± 0.58 | 9.27 ± 0.75# | 7.15 ± 0.66* |
| HR, bmp | 451.7 ± 12.5 | 462.2 ± 14.1 | 477.4 ± 18.1 | 465.3 ± 17.4 |
| LVDd, mm | 3.25 ± 0.14 | 3.31 ± 0.12 | 3.96 ± 0.16# | 3.57 ± 0.13* |
| LVDs, mm | 2.24 ± 0.09 | 2.20 ± 0.11 | 3.15 ± 0.18# | 2.56 ± 0.13* |
| IVS, mm | 0.82 ± 0.03 | 0.81 ± 0.02 | 0.70 ± 0.03# | 0.78 ± 0.04* |
| PW, mm | 0.77 ± 0.05 | 0.76 ± 0.04 | 0.79 ± 0.03 | 0.78 ± 0.02 |
| FS, % | 32.7 ± 1.5 | 33.1 ± 1.2 | 21.3 ± 2.3# | 29.4 ± 2.1* |
| EF, % | 61.3 ± 2.7 | 62.1 ± 2.4 | 44.6 ± 4.8# | 58.2 ± 4.5* |

revealed that I/R injury promoted the formation of fragmented mitochondria with shorter lengths than those of the control group (Fig. 3F–H). Due to increased mitochondrial fission, mitochondrial reactive oxygen species (ROS) levels in CMECs were elevated in the I/R injury group, which was accompanied with an increase in the levels of cytoplasmic ROS levels (Fig. 3I–K). On the other hand, anti-oxidative molecules such as glutathione (GSH), superoxide dismutase (SOD) and glutathione peroxidase (GPX) in CMECs were significantly consumed in the setting of I/R injury (Fig. 3L–N). Due to increased oxidative stress, the mitochondrial membrane potential dissipated (Fig. 3O–P), the mPTP opening rate increased (Fig. 3Q) and caspase-9 was activated in CMECs (Fig. 3R).

Interestingly, empagliflozin treatment suppressed mitochondrial fission and enhanced mitochondrial fusion (Fig. 3F–H), thus normalizing the mitochondrial morphology in I/R-treated CMECs. Empagliflozin also

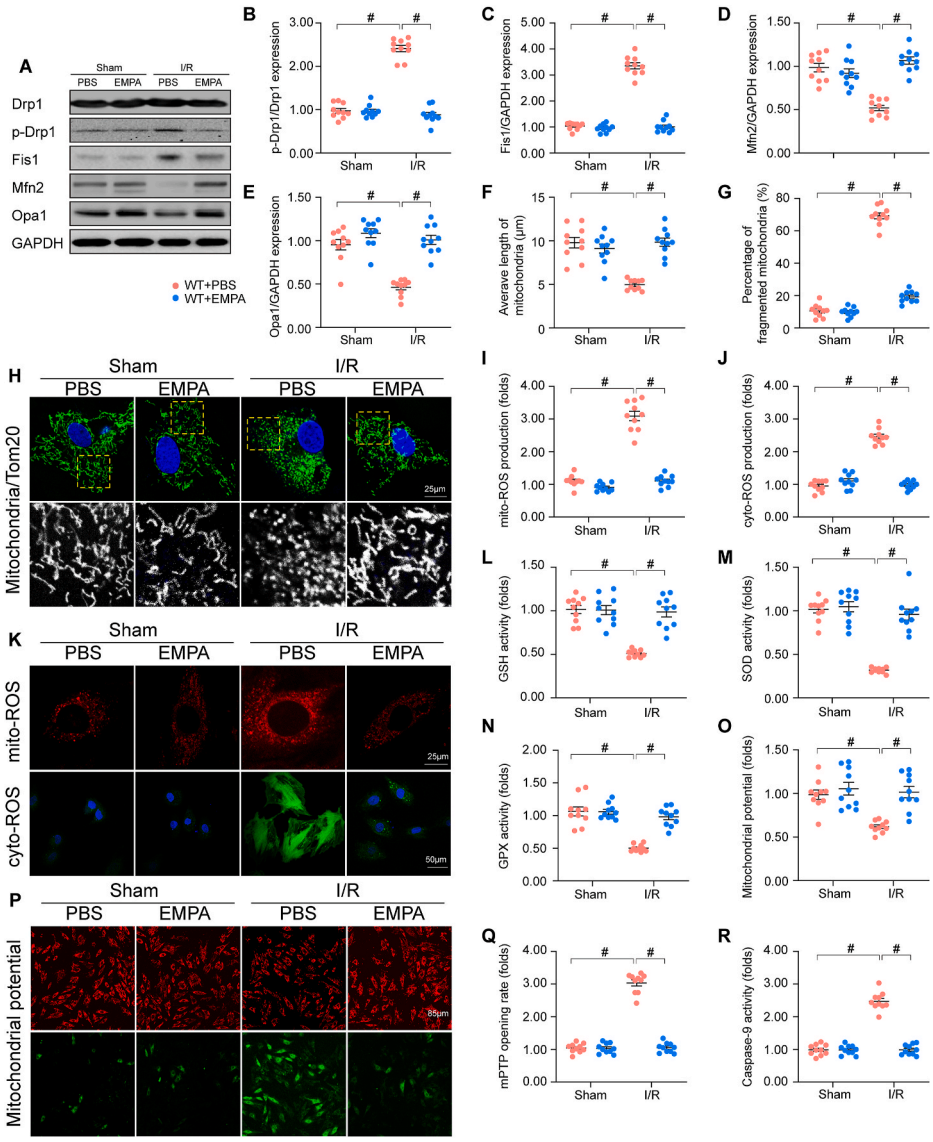


**Fig. 3.** Empagliflozin reduces I/R-induced mitochondrial fission, oxidative stress and apoptosis in CMECs. *In vivo*, mice were assigned to the sham operation group or the myocardial I/R injury group. Empagliflozin (10 mg/kg/d) was administered seven days before myocardial I/R injury. *In vitro*, CMECs were isolated from I/R- or empagliflozin-treated hearts. The cells were cultured for 24 h and then used for functional analyses. **(A–E)** Proteins were isolated from CMECs, and Western blots were used to assess the expression of phosphorylated dynamin-related protein 1 (p-Drp1), Mff, mitochondrial fission 1 (Fis1), mitofusin 2 (Mfn2) and optic atrophy 1 (Opa1). **(F–H)** Immunofluorescence assay of the mitochondrial morphology. The average mitochondrial length was recorded to reflect mitochondrial fission. At least 100 mitochondria from 10 CMECs were used to evaluate the number of CMECs with fragmented mitochondria. **(I–K)** Mitochondrial and cytoplasmic ROS levels in CMECs were determined using immunofluorescence analyses. Mitochondrial ROS were assessed using MitoSOX™ Red, while cytoplasmic ROS were measured using CM-H2DCFDA. **(L–N)** The activity levels of intracellular anti-oxidative molecules such as GSH, SOD and GPX in CMECs were determined using commercially available ELISA kits. **(O–P)** JC-1 staining was used to assess the mitochondrial membrane potential in CMECs. A reduced red-to-green immunosignal of JC-1 indicates an abnormal mitochondrial membrane potential. **(Q)** mPTP opening in CMECs was determined based on the fluorescence intensity of TMRE. **(R)** An ELISA was used to assess capsase-9 levels in CMECs. Experiments were repeated at least three times and the data are shown as mean ± SEM (n = 6 mice or three independent cell isolations per group). *p < 0.05. (For interpretation of the references to colour in this figure legend, the reader is referred to the Web version of this article.)

inhibited mitochondrial ROS production, which accordingly reduced cytoplasmic ROS levels in CMECs following I/R injury (Fig. 3I–K). The anti-oxidative effects of empagliflozin were associated with elevated GSH, SOD and GPX levels in I/R-treated CMECs (Fig. 3L–N), possibly due to reduced mitochondrial ROS generation. Additionally, empagliflozin stabilized the mitochondrial membrane potential and reduced the mPTP opening rate in CMECs following I/R injury, ultimately reducing caspase-9 activation (Fig. 3O–R). Overall, I/R-induced CMEC damage was characterized by disordered mitochondrial dynamics, increased mitochondrial oxidative stress, a reduced mitochondrial membrane potential and enhanced mitochondrial apoptosis. However, empagliflozin attenuated these pathological alterations in CMEC mitochondria.

### *3.4. Empagliflozin activates FUN14 domain-containing 1 (FUNDC1)-dependent mitophagy through the AMPKα1/Unc-51-like autophagy activating kinase 1 (ULK1) pathway*

Mitophagy is a protective mechanism that sustains mitochondrial function and structure [44]. Unfortunately, mitophagy is inhibited during myocardial I/R injury through a complex mechanism [11,22,45]; however, the activation of mitophagy through genetic modifications has been reported to preserve mitochondrial homeostasis and thus protect the cardiac microvasculature against I/R injury [8,11,27,46]. In view of this, we asked whether empagliflozin protected mitochondria and CMECs during I/R by inducing mitophagy. Western blot analysis of mitophagy markers demonstrated that mitochondrial levels of microtubule-associated protein light chain 3-II (mito-LC3II) were reduced in I/R-treated CMECs, whereas p62 accumulation was elevated (Fig. 4A–F). Empagliflozin treatment enhanced mito-LC3II expression and p62 degradation in CMECs following I/R injury.

To confirm these findings, we performed *in vitro* studies in I/R-treated CMECs. The mt-Kemia assay detects acidic mitochondria as a marker of lysosome-engulfed mitochondria. The results of this assay demonstrated that I/R injury inhibited mitophagy in CMECs (Fig. 4G and H), as evidenced by reduced acidic autolysosome formation. However, Empagliflozin promoted mitochondria-lysosome interactions in I/R-treated CMECs (Fig. 4G and H). These data suggested that empagliflozin can induce mitophagy in cardiac microvascular I/R injury.

FUN14 domain-containing 1 (FUNDC1) has been reported to be a critical regulator of mitophagy in cardiac I/R injury [22,47]. The phosphorylation of FUNDC1 by ULK1 was recently revealed to activate FUNDC1-dependent mitophagy [47]. AMPKα1, a downstream effector of empagliflozin [48], is well accepted as the crucial activator of ULK1 [49]. Thus, we speculated that the AMPKα1/ULK1/FUNDC1 signaling

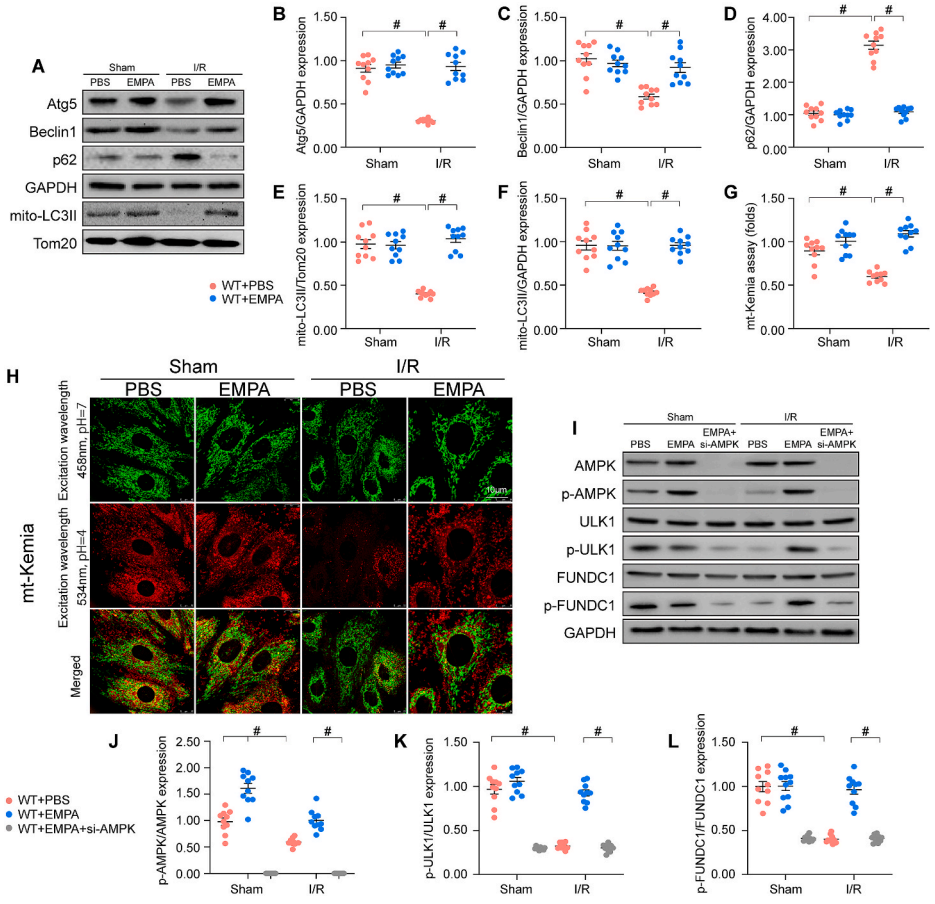


**Fig. 4. Empagliflozin activates FUNDC1-dependent mitophagy through the AMPKα1/ULK1 pathway.** *In vivo*, mice were assigned to the sham operation group or the myocardial I/R injury group. Empagliflozin (10 mg/kg/d) was administered seven days before myocardial I/R injury. *In vitro*, CMECs were isolated from I/R- or empagliflozin-treated hearts. The cells were cultured for 24 h and then used for functional analyses. **(A–F)** Proteins were isolated from reperfused heart tissues, and the levels of mitophagy-related proteins were analyzed through Western blots. **(G–H)** The mt-Kemia assay was used to analyze mitophagy in CMECs. **(I–L)** Proteins were isolated from CMECs, and the levels of p-AMPK, p-ULK1 and p-FUNDC1 were analyzed through Western blots. CC was administered to mice to inhibit empagliflozin-induced AMPK activation. Experiments were repeated at least three times and the data are shown as mean ± SEM (n = 6 mice or three independent cell isolations per group). *p < 0.05.

pathway could be the mechanism whereby empagliflozin induces mitophagy in CMECs. Western blotting demonstrated that I/R injury repressed AMPK phosphorylation and ULK1 expression in CMECs, whereas empagliflozin ameliorated these effects (Fig. 4I-L). Interestingly, when we administered AMPK siRNA to prevent AMPK activation in CMECs in the presence of empagliflozin, both ULK1 and p-FUNDC1 expression were inhibited (Fig. 4I-L). These results suggested that empagliflozin activated mitophagy in I/R-treated CMECs by inducing the AMPKα1/ULK1/FUNDC1 pathway.

### 3.5. *Ablation of FUNDC1 or AMPKα1 abolishes the protective effects of empagliflozin against I/R-induced microvascular damage*

To determine whether empagliflozin attenuated cardiac microvascular I/R injury by inducing the AMPKα1/ULK1/FUNDC1 pathway *in vivo*, we performed loss-of-function experiments for AMPKα1 and FUNDC1. We generated endothelial-specific *AMPKα1*-knockout ($AMPK\alpha1^{EKO}$) mice by crossing $AMPK\alpha1^{f/f}$ mice with $Tie2^{Cre}$ transgenic mice. Similarly, we generated endothelial-specific *FUNDC1*-knockout ($FUNDC1^{EKO}$) mice by crossing $FUNDC1^{f/f}$ mice with $Tie2^{Cre}$ transgenic mice. $Tie2^{Cre}$ mice were used as the control group for both $AMPK\alpha1^{EKO}$ and $FUNDC1^{EKO}$ mice. Empagliflozin was administered to the mice before cardiac I/R injury.

We then used electron microscopy to observe the microvascular structure of reperfused heart tissue from each group. As shown in Fig. 5A, the cardiac microvasculature was more vulnerable to I/R injury in $AMPK\alpha1^{EKO}$ or $FUNDC1^{EKO}$ mice than in $Tie2^{Cre}$ mice, suggesting that AMPKα1 and FUNDC1 are necessary for microvascular protection. Although empagliflozin reduced reperfusion-induced endothelial cell swelling and luminal stenosis, these beneficial effects were negated in $AMPK\alpha1^{EKO}$ and $FUNDC1^{EKO}$ mice (Fig. 5A).

We also performed Western blotting and immunohistochemistry on heart tissues from the various groups of mice. In $Tie2^{Cre}$ mice, I/R injury downregulated p-eNOS and upregulated ET-1 in heart tissue (Fig. 5B–D). Empagliflozin reversed these effects in $Tie2^{Cre}$ mice, but not in $AMPK\alpha1^{EKO}$ or $FUNDC1^{EKO}$ mice (Fig. 5B–D). Similarly, empagliflozin prevented the I/R-induced upregulation of ICAM1 in heart tissue from $Tie2^{Cre}$ mice, but not from $AMPK\alpha1^{EKO}$ or $FUNDC1^{EKO}$ mice (Fig. 5E and F).

We subsequently isolated CMECs from the mice in each group so that endothelial barrier function and integrity could be assessed *in vitro*. As shown in Fig. 5G and H, empagliflozin suppressed FITC-dextran accumulation and increased the TER value in CMECs isolated from I/R-treated $Tie2^{Cre}$ mice, but not from I/R-treated $AMPK\alpha1^{EKO}$ or $FUNDC1^{EKO}$ mice. These findings confirmed that empagliflozin protected cardiac microvessels and endothelial cells against I/R injury by inducing the AMPKα1/ULK1/FUNDC1 pathway.

### 3.6. *Empagliflozin sustains mitochondrial homeostasis in cardiac microvascular endothelial cells by inducing the AMPKα1/ULK1/FUNDC1 pathway*

To verify that empagliflozin maintained endothelial mitochondrial homeostasis by activating the AMPKa1/ULK1/FUNDC1 pathway, we assessed the mitochondrial morphology and structure in freshly isolated CMECs from $Tie2^{Cre}$ mice ($Tie2^{Cre}$-CMECs), $AMPK\alpha1^{EKO}$ mice ($AMPK\alpha1^{EKO}$-CMECs) and $FUNDC1^{EKO}$ mice ($FUNDC1^{EKO}$-CMECs). Immunofluorescence staining (Fig. 6A–C) indicated that I/R injury augmented mitochondrial fission in the $Tie2^{Cre}$-CMEC group, and this effect was exacerbated in the $AMPK\alpha1^{EKO}$-CMEC and $FUNDC1^{EKO}$-CMEC groups. Empagliflozin treatment inhibited I/R-induced pathological mitochondrial division in $Tie2^{Cre}$-CMECs, but not in $AMPK\alpha1^{EKO}$-CMECs

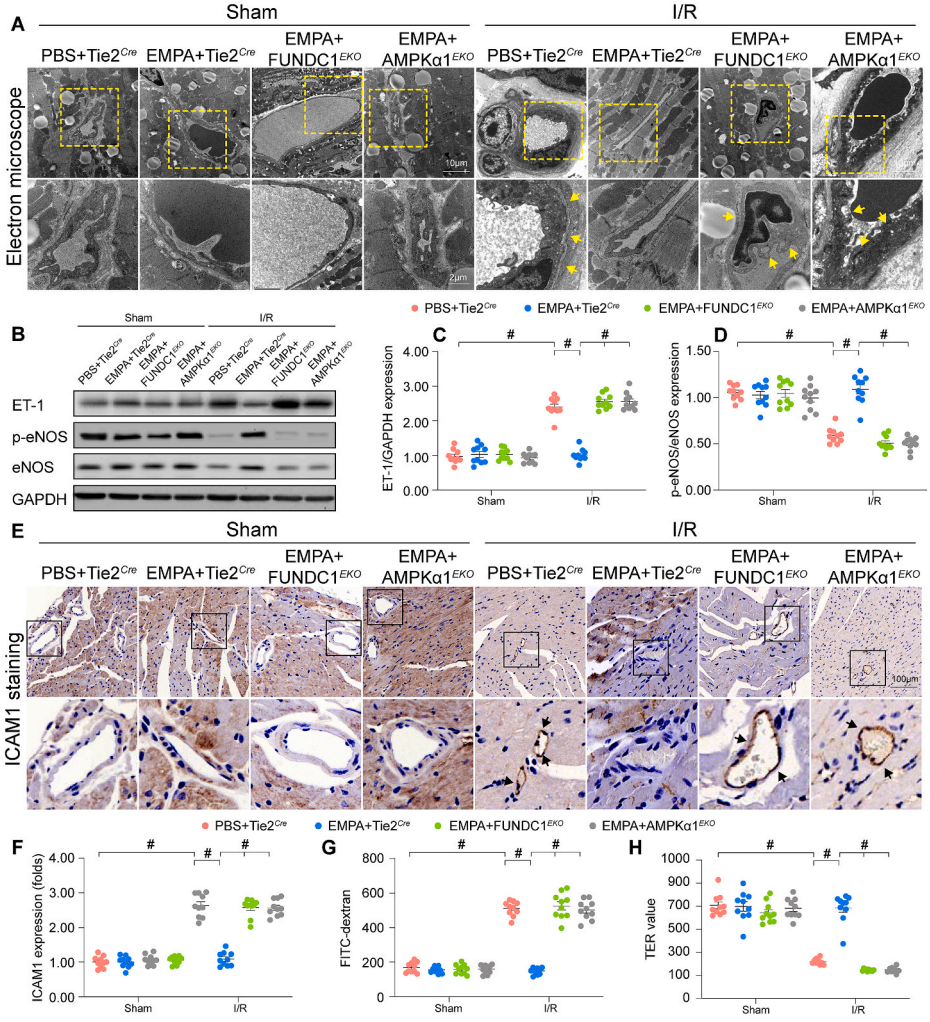


**Fig. 5. Ablation of *FUNDC1* or *AMPKα1* prevents empagliflozin from protecting against I/R-induced microvascular damage.** *In vivo*, AMPKα1$^{EKO}$, FUNDC1$^{EKO}$ or Tie2$^{Cre}$ (control) mice were assigned to the sham operation group or the myocardial I/R injury group. Empagliflozin (10 mg/kg/d) was administered seven days before myocardial I/R injury. **(A)** An electron microscope was used to detect changes in the microvascular structure of the reperfused heart. Yellow arrows indicate microvascular endothelial cell inflation and luminal stenosis. **(B–D)** Proteins were isolated from reperfused heart tissues, and the levels of eNOS and ET-1 were analyzed through Western blots. **(E, F)** Immunohistochemistry assay of ICAM1, an endothelium-specific adhesive factor. **(G, H)** *In vitro*, CMECs were isolated from I/R- or empagliflozin-treated hearts and cultured for 24 h. Then, FITC-dextran clearance and TER assays were used to analyze the endothelial barrier function and integrity of the CMECs. Experiments were repeated at least three times and the data are shown as mean ± SEM (n = 6 mice or three independent cell isolations per group). *p < 0.05. (For interpretation of the references to colour in this figure legend, the reader is referred to the Web version of this article.)

or FUNDC1$^{EKO}$-CMECs. Furthermore, empagliflozin attenuated mitochondrial ROS production (Fig. 6D–F) and enhanced anti-oxidative molecule levels (Fig. 6G–I) under I/R injury in Tie2$^{Cre}$-CMECs, but not in AMPKα1$^{EKO}$-CMECs or FUNDC1$^{EKO}$-CMECs. Similarly, empagliflozin reversed the I/R-induced mitochondrial membrane potential reduction (Fig. 6J and K) in CMECs, but these effects were prevented by the deletion of *AMPKα1* or *FUNDC1*. These data indicated that the activation of the AMPKα1/ULK1/FUNDC1 pathway could be the mechanism whereby empagliflozin sustained mitochondrial homeostasis in CMECs during I/R injury.

## 4. Discussion

Cardiac microvascular I/R injury is a neglected topic in the field of perioperative cardioprotection. The molecular mechanism of I/R-induced microvascular damage is relatively complex, so few drugs are available to protect the cardiac microcirculation during cardiac I/R injury. In the present study, we demonstrated the potential therapeutic value of the AMPKα1/ULK1/FUNDC1 mitophagy pathway for the preservation of endothelial cell homeostasis and microvessel integrity during microvascular I/R injury. We also found that empagliflozin could be considered as an endothelium-specific protective drug that increases the resistance of cardiac microvessels to I/R injury by maintaining endothelial function and structure. Moreover, we discovered that empagliflozin prevented I/R-induced microvascular dysfunction by increasing mitophagy and consequently improving mitochondrial behavior. As far as we know, this is the first study to explore the therapeutic potential of empagliflozin for acute myocardial microvascular impairment. Importantly, these effects of empagliflozin seemed to depend on mitochondrial protection via mitophagy and the AMPK pathway.

The endothelial protective effects of empagliflozin have been described in several in-depth studies. In transverse aortic constriction-induced heart failure, empagliflozin was reported to suppress endothelial apoptosis and maintain capillarization through the Akt/eNOS/nitric oxide pathway, thus increasing heart performance [18,50]. Similarly, empagliflozin was found to inhibit leukocyte-endothelium interactions during diabetes by repressing inflammatory cytokine production [51]. In human coronary artery endothelial cells, empagliflozin exhibited anti-oxidative effects by neutralizing cyclic stretch-induced mitochondrial ROS overproduction, thereby preventing endothelial hyperpermeability [19]. In addition to inhibiting endothelial dysfunction, empagliflozin has been reported to attenuate angiotensin II-induced endothelial senescence by suppressing abnormal activity of the angiotensin II receptor type 1/nicotinamide adenine dinucleotide phosphate oxidase pathway [52,53]. In a murine model of myocardial infarction, empagliflozin was found to reduce the infarct size by increasing the CD31$^{+}$/vascular endothelial growth factor receptor 2$^{+}$ endothelial cell

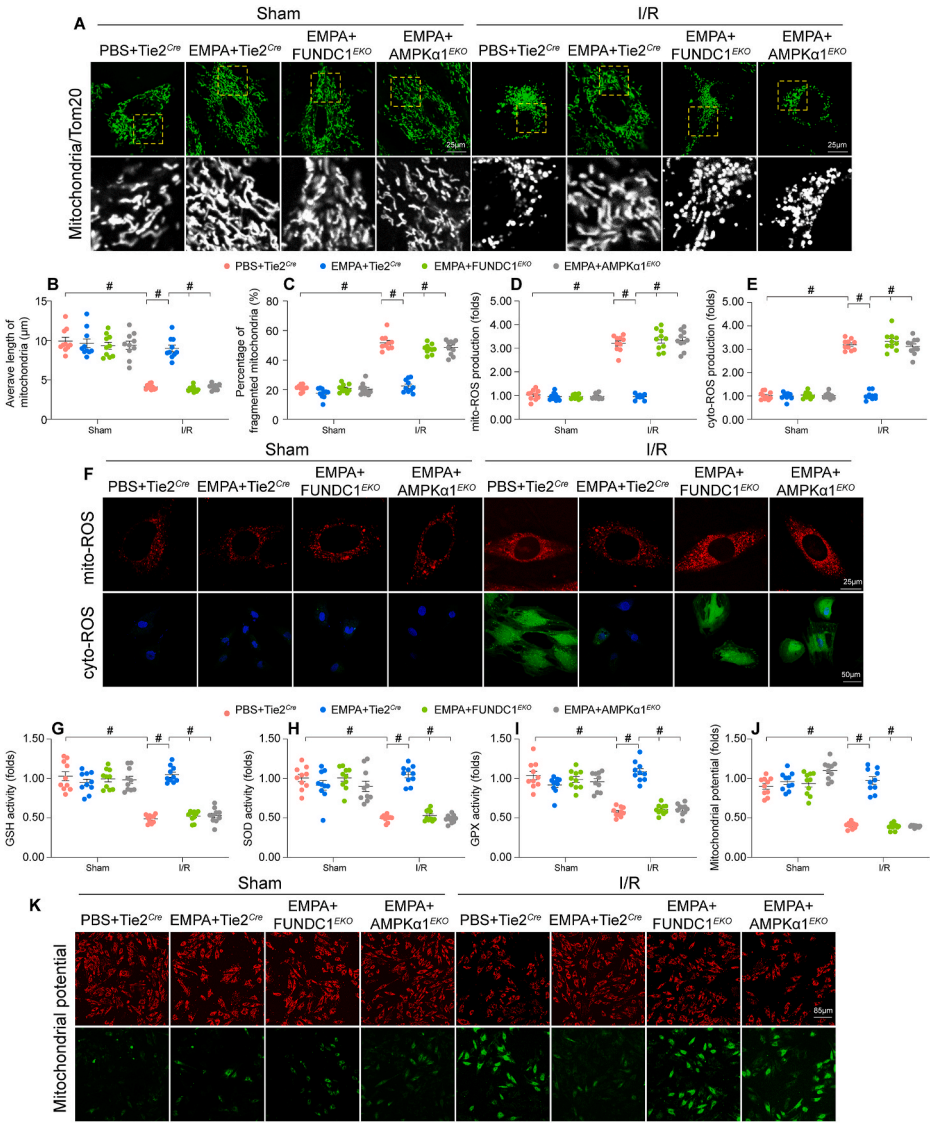


**Fig. 6. Empagliflozin sustains mitochondrial homeostasis in CMECs through the AMPKα1/ULK1/FUNDC1 pathway.** *In vivo*, AMPKα1$^{EKO}$, FUNDC1$^{EKO}$ or Tie2$^{Cre}$ (control) mice were assigned to the sham operation group or the myocardial I/R injury group. Empagliflozin (10 mg/kg/d) was administered seven days before myocardial I/R injury. *In vitro*, CMECs were isolated from I/R- or empagliflozin-treated hearts. The cells were cultured for 24 h and then used for functional analyses. **(A–C)** Immunofluorescence assays were used to assess the mitochondrial morphology in CMECs. The average mitochondrial length was recorded to reflect mitochondrial fission. At least 100 mitochondria from 10 CMECs were used to evaluate the number of CMECs with fragmented mitochondria. **(D–F)** Mitochondrial and cytoplasmic ROS levels in CMECs were determined using immunofluorescence assays. Mitochondrial ROS were assessed using MitoSOX™ Red, while cytoplasmic ROS were measured using CM-H2DCFDA. **(G–I)** The activity levels of intracellular anti-oxidative molecules such as GSH, SOD and GPX in CMECs were determined using commercially available ELISA kits. **(J–K)** JC-1 staining was used to determine the mitochondrial membrane potential in CMECs. A reduced red-to-green immunosignal of JC-1 indicates an abnormal mitochondrial membrane potential. Experiments were repeated at least three times and the data are shown as mean ± SEM (n = 6 mice or three independent cell isolations per group). *p < 0.05. (For interpretation of the references to colour in this figure legend, the reader is referred to the Web version of this article.

ratio (a critical feature of angiogenesis) in the infarcted zone [54]. These studies suggested that empagliflozin activates specific signaling cascades to improve mitochondrial anti-oxidative activity, enhance the anti-inflammatory capacity and induce pro-survival programs in endothelial cells.

In accordance with these previous findings, our *in vitro* and *in vivo* analyses revealed that empagliflozin had pleiotropic effects on endothelial function and structure. Empagliflozin enhanced endothelial integrity, permeability, barrier function and relaxation factor production in the setting of cardiac I/R injury. On the other hand, empagliflozin significantly suppressed endothelial adhesive protein expression and inflammatory responses, thus normalizing local fluid mechanics, maintaining well-organized vessel walls and improving microvascular perfusion. Our study is the first to provide comprehensive evidence that empagliflozin is an effective drug against acute microvascular dysfunction.

Mitochondria serve as sensors of environmental stress and cellular adaptions, in addition to performing their classical functions of glucose metabolism and energy production. Mitochondrial damage contributes to endothelial dysfunction and cardiac microvascular I/R injury [55–57]. Myocardial reperfusion rapidly augments mitochondrial fission factor (Mff)-induced mitochondrial fission, resulting in mtDNA damage and endothelial oxidative stress [7]. Moreover, reperfusion activates mitochondrial apoptosis by inducing mitochondrial membrane hyperpermeability, mPTP opening and cytochrome c leakage [27,58]. Consistently, we found that mitochondrial fission was activated and fusion was suppressed in I/R-treated CMECs. Due to these mitochondrial morphological alterations, mitochondrial oxidative stress was induced, the mitochondrial membrane potential was reduced and apoptosis markers were upregulated.

Mitophagy is regarded as an important repair mechanism for damaged and dysfunctional mitochondria through normalization of mitochondrial fission/fusion [59]. Increased mitochondrial fission and/or decreased mitochondrial fusion promotes the formation of fragmented mitochondria which promotes cellular oxidative stress or release pro-apoptotic factors (such as cytochrome c) into the cytoplasm where the mitochondria-dependent apoptosis is induced [9,60–62]. Mitophagy promotes the removal of fragmented mitochondria and therefore play anti-oxidative and/or anti-apoptotic roles in endothelial cells [11,63]. However, at the stage of myocardial reperfusion, mitophagy is largely suppressed due to multiple mechanisms [11,22,45,64]. Interestingly, we found that empagliflozin restored mitophagy by inducing the AMPKa1/ULK1/FUNDC1 pathway during I/R injury, thus reducing mitochondrial damage in CMECs. Genetic ablation of *FUNDC1* or *AMPKα1* prevented empagliflozin from inhibiting mitochondrial oxidative stress, stabilizing the mitochondrial membrane potential and

suppressing mitochondrial apoptosis in CMECs. These findings demonstrated that empagliflozin maintained endothelial mitochondrial performance primarily by preserving mitophagy under I/R injury.

It is well documented that the intracellular effectors of empagliflozin include extracellular signal-regulated kinase 1/2 [65], phosphoinositide 3-kinase/Akt [18], transforming growth factor β1 [66], nuclear factor κB [67], Janus kinase 2 [67], Sirtuin 1 [68], hypoxia inducible factor 1α [69], protein kinase G Iα [70], heme oxygenase 1 [71], peroxisome proliferator-activated receptor gamma coactivator 1α [72] and AMPKα1 [20]. Among them, AMPK has been identified as an indispensable inducer of mitophagy. Reduced energy production increases AMP levels and thus promotes the phosphorylation of AMPKα1, which directly activates ULK1 by phosphorylating it at Ser317 or Ser777 [73]. Upon its activation, ULK1 translocates to the mitochondrial outer membrane surface to phosphorylate FUNDC1 at Ser17 [47], thus inducing mitophagy. The ULK1/FUNDC1 pathway has been characterized as a protective mechanism under various pathological conditions, including renal I/R injury [47], hypoxia-related nerve cell apoptosis [74] and myocardial I/R injury [75].

In the present study, we demonstrated that empagliflozin stimulated ULK1/FUNDC1-dependent mitophagy by activating AMPKα1. This is the first evidence of a relationship between empagliflozin and the AMPKα1/ULK1/FUNDC1 mitophagy pathway. Our *in vivo* genetic deletion experiments and biochemical studies solidly confirmed that this pathway improved endothelial cell function and microvascular integrity. Thus, the AMPKα1/ULK1/FUNDC1 mitophagy pathway may be an endothelium-specific orchestrator of the cellular response to empagliflozin in the pathogenesis of cardiac microvascular I/R injury. However, there are several limitations in the present study. First, although we demonstrated the protective effects of empagliflozin on microvascular structure, there is no direct evidence to show the influence of empagliflozin on microvascular function *in vivo*. Coronary flow reserve (CFR) is an important evaluator for assessing cardiac microcirculation function *in vivo* and therefore it requires additional experiments to further validate the impact of empagliflozin on microvascular function. Second, although we reported the roles of empagliflozin in regulating mitochondrial fission/fusion and mitophagy in I/R-induced cardiac microvascular damage, the complex relationships between mitochondrial fusion/fission and mitophagy in the presence of empagliflozin need further investigation.

## 5. Conclusions

Overall, our study revealed the mechanism whereby empagliflozin inhibits reperfusion-induced cardiac microvascular damage: namely, by activating AMPKα1 and thus augmenting FUNDC1-dependent mitophagy through ULK1 phosphorylation. Increased mitophagy normalizes mitochondrial fission/fusion, reduces endothelial oxidative stress and hampers mitochondrial apoptotic signaling, thereby improving endothelial function and microvascular structure. Our discovery of the links between empagliflozin, the AMPKα1/ULK1/FUNDC1/mitophagy axis and endothelial protection will enable the exploration of new treatment targets and drugs for cardiac microvascular I/R injury. Clinical trials are urgently needed to affirm our observations for the benefit of patients with acute microvascular dysfunction.

## Author's contributions

YT, ZZG, XC and ZYL contributed to the study designation. YT, FW JH and ST performed experiments and data analysis. TTC, KRW, NXS and HZ contributed to manuscript writing and editing. DM, CC, XC and YT conducted a critical revision of the manuscript. All authors approved the final manuscript.

## Funding

This study is supported by the National Natural Science Foundation of China (NO.82102262, NO.82170241, NO.81900252) and Guangdong Basic and Applied Basic Research Foundation (NO. 2021A1515010977 and NO. 2020A1515110174).

## Availability of data and materials

All data generated or analyzed during this study are included in this published article.

## Declaration of competing interest

The authors have declared that they have no conflicts of interest.

## Acknowledgements

None.

## Abbreviations

| | |
|---|---|
| ULK1 | Unc-51-like autophagy activating kinase 1 |
| AMPKα1 | adenosine monophosphate-activated protein kinase catalytic subunit alpha 1 |
| FUNDC1 | FUN14 domain-containing 1 |
| I/R | ischemia/reperfusion |
| mPTP | mitochondrial permeability transition pore |
| mtDNA | mitochondrial DNA |
| AMP | adenosine monophosphate |
| ATP | adenosine triphosphate |
| TNFα | tumor necrosis factor α |
| MCP1 | monocyte chemotactic protein 1 |
| IL-6 | interleukin 6 |

## References

[1] M. Yildiz, S.R. Wade, T.D. Henry, STEMI Care 2021: Addressing the Knowledge Gaps, Am Heart J Plus, 2021, p. 100044.
[2] H. Kakavand, M. Aghakouchakzadeh, J.C. Coons, A.H. Talasaz, Pharmacologic prevention of myocardial ischemia-reperfusion injury in patients with acute coronary syndrome undergoing percutaneous coronary intervention, J. Cardiovasc. Pharmacol. 77 (4) (2021) 430–449.
[3] S.M. Davidson, P. Ferdinandy, I. Andreadou, H.E. Bøtker, G. Heusch, B. Ibáñez, M. Ovize, R. Schulz, D.M. Yellon, D.J. Hausenloy, D. Garcia-Dorado, Multitarget strategies to reduce myocardial ischemia/reperfusion injury: JACC review topic of the week, J. Am. Coll. Cardiol. 73 (1) (2019) 89–99.
[4] J. Wang, S. Toan, H. Zhou, New insights into the role of mitochondria in cardiac microvascular ischemia/reperfusion injury, Angiogenesis 23 (3) (2020) 299–314.
[5] J. Wang, S. Toan, H. Zhou, Mitochondrial quality control in cardiac microvascular ischemia-reperfusion injury: new insights into the mechanisms and therapeutic potentials, Pharmacol. Res. 156 (2020) 104771.
[6] X. Chang, A. Lochner, H.H. Wang, S. Wang, H. Zhu, J. Ren, H. Zhou, Coronary microvascular injury in myocardial infarction: perception and knowledge for mitochondrial quality control, Theranostics 11 (14) (2021) 6766–6785.
[7] H. Zhou, S. Hu, Q. Jin, C. Shi, Y. Zhang, P. Zhu, Q. Ma, F. Tian, Y. Chen, Mff-dependent mitochondrial fission contributes to the pathogenesis of cardiac microvasculature ischemia/reperfusion injury via induction of mROS-mediated cardiolipin oxidation and HK2/VDAC1 disassociation-involved mPTP opening, J. Am. Heart Assoc. 6 (3) (2017).
[8] H. Zhou, Y. Zhang, S. Hu, C. Shi, P. Zhu, Q. Ma, Q. Jin, F. Cao, F. Tian, Y. Chen, Melatonin protects cardiac microvasculature against ischemia/reperfusion injury via suppression of mitochondrial fission-VDAC1-HK2-mPTP-mitophagy axis, J. Pineal Res. 63 (1) (2017).
[9] H. Zhou, C. Shi, S. Hu, H. Zhu, J. Ren, Y. Chen, BI1 is associated with microvascular protection in cardiac ischemia reperfusion injury via repressing Syk-Nox2-Drp1-mitochondrial fission pathways, Angiogenesis 21 (3) (2018) 599–615.
[10] H. Zhou, J. Wang, P. Zhu, S. Hu, J. Ren, Ripk3 regulates cardiac microvascular reperfusion injury: the role of IP3R-dependent calcium overload, XO-mediated oxidative stress and F-action/filopodia-based cellular migration, Cell. Signal. 45 (2018) 12–22.
[11] H. Zhou, J. Wang, P. Zhu, H. Zhu, S. Toan, S. Hu, J. Ren, Y. Chen, NR4A1 aggravates the cardiac microvascular ischemia reperfusion injury through suppressing FUNDC1-mediated mitophagy and promoting Mff-required mitochondrial fission by CK2alpha, Basic Res. Cardiol. 113 (4) (2018) 23.

[12] H. Jin, Y. Zhu, Y. Li, X. Ding, W. Ma, X. Han, B. Wang, BDNF-mediated mitophagy alleviates high-glucose-induced brain microvascular endothelial cell injury, Apoptosis 24 (5–6) (2019) 511–528.

[13] X. Luo, S. Cai, Y. Li, G. Li, Y. Cao, C. Ai, Y. Gao, T. Li, Drp-1 as potential therapeutic target for lipopolysaccharide-induced vascular hyperpermeability, Oxid. Med. Cell. Longev. 2020 (2020) 5820245.

[14] X. Luo, R. Liu, Z. Zhang, Z. Chen, J. He, Y. Liu, Mitochondrial division inhibitor 1 attenuates mitophagy in a rat model of acute lung injury, BioMed Res. Int. 2019 (2019) 2193706.

[15] K. Khunti, SGLT2 inhibitors in people with and without T2DM, Nat. Rev. Endocrinol. 17 (2) (2021) 75–76.

[16] B. Zinman, C. Wanner, J.M. Lachin, D. Fitchett, E. Bluhmki, S. Hantel, M. Mattheus, T. Devins, O.E. Johansen, H.J. Woerle, U.C. Broedl, S.E. Inzucchi, Empagliflozin, cardiovascular outcomes, and mortality in type 2 diabetes, N. Engl. J. Med. 373 (22) (2015) 2117–2128.

[17] S.A. Hawley, R.J. Ford, B.K. Smith, G.J. Gowans, S.J. Mancini, R.D. Pitt, E.A. Day, I.P. Salt, G.R. Steinberg, D.G. Hardie, The Na+/Glucose cotransporter inhibitor canagliflozin activates AMPK by inhibiting mitochondrial function and increasing cellular AMP levels, Diabetes 65 (9) (2016) 2784–2794.

[18] M. Nakao, I. Shimizu, G. Katsuumi, Y. Yoshida, M. Suda, Y. Hayashi, R. Ikegami, Y. T. Hsiao, S. Okuda, T. Soga, T. Minamino, Empagliflozin maintains capillarization and improves cardiac function in a murine model of left ventricular pressure overload, Sci. Rep. 11 (1) (2021) 18384.

[19] X. Li, G. Römer, R.P. Kerindongo, J. Hermanides, M. Albrecht, M.W. Hollmann, C. J. Zuurbier, B. Preckel, N.C. Weber, Sodium glucose Co-transporter 2 inhibitors ameliorate endothelium barrier dysfunction induced by cyclic stretch through inhibition of reactive oxygen species, Int. J. Mol. Sci. 22 (11) (2021).

[20] H. Zhou, S. Wang, P. Zhu, S. Hu, Y. Chen, J. Ren, Empagliflozin rescues diabetic myocardial microvascular injury via AMPK-mediated inhibition of mitochondrial fission, Redox Biol 15 (2018) 335–346.

[21] S.R. Yurista, H.H.W. Silljé, M. Rienstra, R.A. De Boer, B.D. Westenbrink, Sodium-glucose co-transporter 2 inhibition as a mitochondrial therapy for atrial fibrillation in patients with diabetes? Cardiovasc. Diabetol. 19 (1) (2020) 5.

[22] H. Zhou, P. Zhu, J. Wang, H. Zhu, J. Ren, Y. Chen, Pathogenesis of cardiac ischemia reperfusion injury is associated with CK2alpha-disturbed mitochondrial homeostasis via suppression of FUNDC1-related mitophagy, Cell Death Differ 25 (6) (2018) 1080–1093.

[23] H. Ge, W. Lin, Z. Lou, R. Chen, H. Shi, Q. Zhao, Z. Lin, Catalpol alleviates myocardial ischemia reperfusion injury by activating the Nrf2/HO-1 signaling pathway, Microvasc. Res. (2021) 104302.

[24] P. Zhu, S. Hu, Q. Jin, D. Li, F. Tian, S. Toan, Y. Li, H. Zhou, Y. Chen, Ripk3 promotes ER stress-induced necroptosis in cardiac IR injury: a mechanism involving calcium overload/XO/ROS/mPTP pathway, Redox Biol 16 (2018) 157–168.

[25] Q. Jin, R. Li, N. Hu, T. Xin, P. Zhu, S. Hu, S. Ma, H. Zhu, J. Ren, H. Zhou, DUSP1 alleviates cardiac ischemia/reperfusion injury by suppressing the Mff-required mitochondrial fission and Bnip3-related mitophagy via the JNK pathways, Redox Biol 14 (2018) 576–587.

[26] Y. Zhang, H. Zhou, W. Wu, C. Shi, S. Hu, T. Yin, Q. Ma, T. Han, Y. Zhang, F. Tian, Y. Chen, Liraglutide protects cardiac microvascular endothelial cells against hypoxia/reoxygenation injury through the suppression of the SR-Ca(2+)-XO-ROS axis via activation of the GLP-1R/PI3K/Akt/survivin pathways, Free Radic. Biol. Med. 95 (2016) 278–292.

[27] Y. Tan, D. Mui, S. Toan, P. Zhu, R. Li, H. Zhou, SERCA overexpression improves mitochondrial quality control and attenuates cardiac microvascular ischemia-reperfusion injury, Mol. Ther. Nucleic Acids 22 (2020) 696–707.

[28] D. Maier-Begandt, H.S. Comstra, S.A. Molina, N. Krüger, C.A. Ruddiman, Y.L. Chen, X. Chen, L.A. Biwer, S.R. Johnstone, A.W. Lohman, M.E. Good, L.J. Delalio, K. Hong, H.M. Bacon, Z. Yan, S.K. Sonkusare, M. Koval, B.E. Isakson, A venous-specific purinergic signaling cascade initiated by Pannexin 1 regulates TNFα-induced increases in endothelial permeability, Sci. Signal. 14 (672) (2021).

[29] S. Huang, Z. Li, Z. Wu, C. Liu, M. Yu, M. Wen, L. Zhang, X. Wang, DDAH2 suppresses RLR-MAVS-mediated innate antiviral immunity by stimulating nitric oxide-activated, Drp1-induced mitochondrial fission, Sci. Signal. 14 (678) (2021).

[30] H. Zhou, J. Wang, S. Hu, H. Zhu, S. Toanc, J. Ren, BI1 alleviates cardiac microvascular ischemia-reperfusion injury via modifying mitochondrial fission and inhibiting XO/ROS/F-actin pathways, J. Cell. Physiol. 234 (4) (2019) 5056–5069.

[31] G.S. Gunaratne, E. Brailoiu, S. He, E.M. Unterwald, S. Patel, J.T. Slama, T. F. Walseth, J.S. Marchant, Essential requirement for JPT2 in NAADP-evoked Ca(2+) signaling, Sci. Signal. 14 (675) (2021).

[32] Y. Fichman, R.J. Myers Jr., D.G. Grant, R. Mittler, Plasmodesmata-localized proteins and ROS orchestrate light-induced rapid systemic signaling in Arabidopsis, Sci. Signal. 14 (671) (2021).

[33] J. Wang, P. Zhu, S. Toan, R. Li, J. Ren, H. Zhou, Pum2-Mff axis fine-tunes mitochondrial quality control in acute ischemic kidney injury, Cell Biol. Toxicol. 36 (4) (2020) 365–378.

[34] S. Feno, F. Munari, D.V. Reane, R. Gissi, D.H. Hoang, A. Castegna, B. Chazaud, A. Viola, R. Rizzuto, A. Raffaello, The dominant-negative mitochondrial calcium uniporter subunit MCUb drives macrophage polarization during skeletal muscle regeneration, Sci. Signal. 14 (707) (2021), eabf3838.

[35] H. Zhou, S. Toan, P. Zhu, J. Wang, J. Ren, Y. Zhang, DNA-PKcs promotes cardiac ischemia reperfusion injury through mitigating BI-1-governed mitochondrial homeostasis, Basic Res. Cardiol. 115 (2) (2020) 11.

[36] O. Ernst, J. Sun, B. Lin, B. Banoth, M.G. Dorrington, J. Liang, B. Schwarz, K. A. Stromberg, S. Katz, S.J. Vayttaden, C.J. Bradfield, N. Slepushkina, C.M. Rice, E. Buehler, J.S. Khillan, D.W. Mcvicar, C.M. Bosio, C.E. Bryant, F.S. Sutterwala, S. E. Martin, M. Lal-Nag, I.D.C. Fraser, A genome-wide screen uncovers multiple roles for mitochondrial nucleoside diphosphate kinase D in inflammasome activation, Sci. Signal. 14 (694) (2021).

[37] D.R. Crooks, N. Maio, M. Lang, C.J. Ricketts, C.D. Vocke, S. Gurram, S. Turan, Y. Y. Kim, G.M. Cawthon, F. Sohelian, N. De Val, R.M. Pfeiffer, P. Jailwala, M. Tandon, B. Tran, T.W. Fan, A.N. Lane, T. Ried, D. Wangsa, A.A. Malayeri, M. J. Merino, Y. Yang, J.L. Meier, M.W. Ball, T.A. Rouault, R. Srinivasan, W. M. Linehan, Mitochondrial DNA alterations underlie an irreversible shift to aerobic glycolysis in fumarate hydratase-deficient renal cancer, Sci. Signal. 14 (664) (2021).

[38] H. Abe, Y. Tanada, S. Omiya, M.N. Podaru, T. Murakawa, J. Ito, A.M. Shah, S. J. Conway, M. Ono, K. Otsu, NF-κB activation in cardiac fibroblasts results in the recruitment of inflammatory Ly6C(hi) monocytes in pressure-overloaded hearts, Sci. Signal. 14 (704) (2021), eabe4932.

[39] R.C. Coleman, A. Eguchi, M. Lieu, R. Roy, E.W. Barr, J. Ibetti, A.M. Lucchese, A. M. Peluzzo, K. Gresham, J.K. Chuprun, W.J. Koch, A peptide of the N terminus of GRK5 attenuates pressure-overload hypertrophy and heart failure, Sci. Signal. 14 (676) (2021).

[40] J. Wang, P. Zhu, R. Li, J. Ren, Y. Zhang, H. Zhou, Bax inhibitor 1 preserves mitochondrial homeostasis in acute kidney injury through promoting mitochondrial retention of PHB2, Theranostics 10 (1) (2020) 384–397.

[41] Y. Mao, M.L. Kleinjan, I. Jilishitz, B. Swaminathan, H. Obinata, Y.A. Komarova, K. J. Bayless, T. Hla, J.K. Kitajewski, CLIC1 and CLIC4 mediate endothelial S1P receptor signaling to facilitate Rac1 and RhoA activity and function, Sci. Signal. 14 (679) (2021).

[42] S. Li, J. Chen, M. Liu, Y. Chen, Y. Wu, Q. Li, T. Ma, J. Gao, Y. Xia, M. Fan, A. Chen, D. Lu, E. Su, F. Xu, Z. Chen, J. Qian, J. Ge, Protective effect of HINT2 on mitochondrial function via repressing MCU complex activation attenuates cardiac microvascular ischemia-reperfusion injury, Basic Res. Cardiol. 116 (1) (2021) 65.

[43] F. Tian, Y. Zhang, Overexpression of SERCA2a alleviates cardiac microvascular ischemic injury by suppressing mfn2-mediated ER/mitochondrial calcium tethering, Front. Cell Dev. Biol. 9 (2021) 636553.

[44] A. Tripathi, G. Scaini, T. Barichello, J. Quevedo, A. Pillai, Mitophagy in depression: pathophysiology and treatment targets, Mitochondrion 61 (2021) 1–10.

[45] H. Wu, M. Ye, D. Liu, J. Yang, J.W. Ding, J. Zhang, X.A. Wang, W.S. Dong, Z.X. Fan, J. Yang, UCP2 protect the heart from myocardial ischemia/reperfusion injury via induction of mitochondrial autophagy, J. Cell. Biochem. 120 (9) (2019) 15455–15466.

[46] H. Zhou, D. Li, P. Zhu, S. Hu, N. Hu, S. Ma, Y. Zhang, T. Han, J. Ren, F. Cao, Y. Chen, Melatonin suppresses platelet activation and function against cardiac ischemia/reperfusion injury via PPARgamma/FUNDC1/mitophagy pathways, J. Pineal Res. 63 (4) (2017).

[47] J. Wang, P. Zhu, R. Li, J. Ren, H. Zhou, Fundc1-dependent mitophagy is obligatory to ischemic preconditioning-conferred renoprotection in ischemic AKI via suppression of Drp1-mediated mitochondrial fission, Redox Biol 30 (2020) 101415.

[48] S.J. Mancini, D. Boyd, O.J. Katwan, A. Strembitska, T.A. Almabrouk, S. Kennedy, T. M. Palmer, I.P. Salt, Canagliflozin inhibits interleukin-1β-stimulated cytokine and chemokine secretion in vascular endothelial cells by AMP-activated protein kinase-dependent and -independent mechanisms, Sci. Rep. 8 (1) (2018) 5276.

[49] C.M. Hung, P.S. Lombardo, N. Malik, S.N. Brun, K. Hellberg, J.L. Van Nostrand, D. Garcia, J. Baumgart, K. Diffenderfer, J.M. Asara, R.J. Shaw, AMPK/ULK1-mediated phosphorylation of Parkin ACT domain mediates an early step in mitophagy, Sci. Adv. 7 (15) (2021).

[50] L. Marongiu, F. Mingozzi, C. Cigni, R. Marzi, M. Di Gioia, M. Garrè, D. Parazzoli, L. Sironi, M. Collini, R. Sakaguchi, T. Morii, M. Crosti, M. Moro, S. Schurmans, T. Catelani, R. Rotem, M. Colombo, S. Shears, D. Prosperi, I. Zanoni, F. Granucci, Inositol 1,4,5-trisphosphate 3-kinase B promotes Ca(2+) mobilization and the inflammatory activity of dendritic cells, Sci. Signal. 14 (676) (2021).

[51] F. Canet, F. Iannantuoni, A.M. Marañon, P. Díaz-Pozo, S. López-Domènech, T. Vezza, B. Navarro, E. Solá, R. Falcón, C. Bañuls, C. Morillas, M. Rocha, V. M. Víctor, Does empagliflozin modulate leukocyte-endothelium interactions, oxidative stress, and inflammation in type 2 diabetes? Antioxidants 10 (8) (2021).

[52] S.H. Park, E. Belcastro, H. Hasan, K. Matsushita, B. Marchandot, M. Abbas, F. Toti, C. Auger, L. Jesel, P. Ohlmann, O. Morel, V.B. Schini-Kerth, Angiotensin II-induced upregulation of SGLT1 and 2 contributes to human microparticle-stimulated endothelial senescence and dysfunction: protective effect of gliflozins, Cardiovasc. Diabetol. 20 (1) (2021) 65.

[53] M.G. Mccoy, D.W. Nascimento, M. Veleeparambil, R. Murtazina, D. Gao, S. Tkachenko, E. Podrez, T.V. Byzova, Endothelial TLR2 promotes proangiogenic immune cell recruitment and tumor angiogenesis, Sci. Signal. 14 (666) (2021).

[54] P.E. Nikolaou, P. Efentakis, F. Abu Qourah, S. Femminò, M. Makridakis, Z. Kanaki, A. Varela, M. Tsoumani, C.H. Davos, C.A. Dimitriou, A. Tasouli, G. Dimitriadis, N. Kostomitsopoulos, C.J. Zuurbier, A. Vlahou, A. Klinakis, M.F. Brizzi, E. K. Iliodromitis, I. Andreadou, Chronic empagliflozin treatment reduces myocardial infarct size in nondiabetic mice through STAT-3-mediated protection on microvascular endothelial cells and reduction of oxidative stress, Antioxidants Redox Signal. 34 (7) (2021) 551–571.

[55] H. Zhu, S. Toan, D. Mui, H. Zhou, Mitochondrial quality surveillance as a therapeutic target in myocardial infarction, Acta Physiol. 231 (3) (2021), e13590.

[56] H. Zhou, J. Ren, S. Toan, D. Mui, Role of mitochondrial quality surveillance in myocardial infarction: from bench to bedside, Ageing Res. Rev. 66 (2021) 101250.

[57] J. Wang, H. Zhou, Mitochondrial quality control mechanisms as molecular targets in cardiac ischemia-reperfusion injury, Acta Pharm. Sin. B 10 (10) (2020) 1866–1879.

[58] C.C. Rada, H. Mejia-Pena, N.J. Grimsey, I. Canto Cordova, J. Olson, J.M. Wozniak, D.J. Gonzalez, V. Nizet, J. Trejo, Heat shock protein 27 activity is linked to

endothelial barrier recovery after proinflammatory GPCR-induced disruption, Sci. Signal. 14 (698) (2021), eabc1044.
[59] W. Zhang, S. Siraj, R. Zhang, Q. Chen, Mitophagy receptor FUNDC1 regulates mitochondrial homeostasis and protects the heart from I/R injury, Autophagy 13 (6) (2017) 1080–1081.
[60] Y. Song, H. Xing, Y. He, Z. Zhang, G. Shi, S. Wu, Y. Liu, E.O. Harrington, F. W. Sellke, J. Feng, Inhibition of mitochondrial reactive oxygen species improves coronary endothelial function after cardioplegic hypoxia/reoxygenation, J. Thorac. Cardiovasc. Surg. (2021).
[61] Y. Chen, C. Liu, P. Zhou, J. Li, X. Zhao, Y. Wang, R. Chen, L. Song, H. Zhao, H. Yan, Coronary endothelium No-reflow injury is associated with ROS-modified mitochondrial fission through the JNK-drp1 signaling pathway, Oxid. Med. Cell. Longev. 2021 (2021) 6699516.
[62] L.F. Ribeiro, T. Catarino, M. Carvalho, L. Cortes, S.D. Santos, P.O. Opazo, L. R. Ribeiro, B. Oliveiros, D. Choquet, J.A. Esteban, J. Peça, A.L. Carvalho, Ligand-independent activity of the ghrelin receptor modulates AMPA receptor trafficking and supports memory formation, Sci. Signal. 14 (670) (2021).
[63] D. Wu, H. Ji, W. Du, L. Ren, G. Qian, Mitophagy alleviates ischemia/reperfusion-induced microvascular damage through improving mitochondrial quality control, Bioengineered 13 (2) (2022) 3596–3607.
[64] S. Raza, E. Jokl, J. Pritchett, K. Martin, K. Su, K. Simpson, L. Birchall, A.F. Mullan, V.S. Athwal, D.T. Doherty, L. Zeef, N.C. Henderson, P.A. Kalra, N.A. Hanley, K. Piper Hanley, SOX9 is required for kidney fibrosis and activates NAV3 to drive renal myofibroblast function, Sci. Signal. 14 (672) (2021).
[65] Z. Hu, F. Ju, L. Du, G.W. Abbott, Empagliflozin protects the heart against ischemia/reperfusion-induced sudden cardiac death, Cardiovasc. Diabetol. 20 (1) (2021) 199.
[66] E. Daud, O. Ertracht, N. Bandel, G. Moady, M. Shehadeh, T. Reuveni, S. Atar, The impact of empagliflozin on cardiac physiology and fibrosis early after myocardial infarction in non-diabetic rats, Cardiovasc. Diabetol. 20 (1) (2021) 132.
[67] N. Lee, Y.J. Heo, S.E. Choi, J.Y. Jeon, S.J. Han, D.J. Kim, Y. Kang, K.W. Lee, H. J. Kim, Anti-inflammatory effects of empagliflozin and gemigliptin on LPS-stimulated macrophage via the IKK/NF-κB, MKK7/JNK, and JAK2/STAT1 signalling pathways, J. Immunol. Res. 2021 (2021) 9944880.
[68] G. Tian, Y. Yu, H. Deng, L. Yang, X. Shi, B. Yu, Empagliflozin alleviates ethanol-induced cardiomyocyte injury through inhibition of mitochondrial apoptosis via a SIRT1/PTEN/Akt pathway, Clin. Exp. Pharmacol. Physiol. 48 (6) (2021) 837–845.
[69] R.G. Abdel-Latif, R.A. Rifaai, E.F. Amin, Empagliflozin alleviates neuronal apoptosis induced by cerebral ischemia/reperfusion injury through HIF-1α/VEGF signaling pathway, Arch Pharm. Res. (Seoul) 43 (5) (2020) 514–525.
[70] D. Kolijn, S. Pabel, Y. Tian, M. Lódi, M. Herwig, A. Carrizzo, S. Zhazykbayeva, Á. Kovács, G. Fülöp, I. Falcão-Pires, P.H. Reusch, S.V. Linthout, Z. Papp, L. Van Heerebeek, C. Vecchione, L.S. Maier, M. Ciccarelli, C. Tschöpe, A. Mügge, Z. Bagi, S. Sossalla, N. Hamdani, Empagliflozin improves endothelial and cardiomyocyte function in human heart failure with preserved ejection fraction via reduced pro-inflammatory-oxidative pathways and protein kinase Gα oxidation, Cardiovasc. Res. 117 (2) (2021) 495–507.
[71] G. Behnammanesh, G.L. Durante, Y.P. Khanna, K.J. Peyton, W. Durante, Canagliflozin inhibits vascular smooth muscle cell proliferation and migration: role of heme oxygenase-1, Redox Biol 32 (2020) 101527.
[72] Q. Shao, L. Meng, S. Lee, G. Tse, M. Gong, Z. Zhang, J. Zhao, Y. Zhao, G. Li, T. Liu, Empagliflozin, a sodium glucose co-transporter-2 inhibitor, alleviates atrial remodeling and improves mitochondrial function in high-fat diet/streptozotocin-induced diabetic rats, Cardiovasc. Diabetol. 18 (1) (2019) 165.
[73] J. Kim, M. Kundu, B. Viollet, K.L. Guan, AMPK and mTOR regulate autophagy through direct phosphorylation of Ulk1, Nat. Cell Biol. 13 (2) (2011) 132–141.
[74] L. Wang, P. Wang, H. Dong, S. Wang, H. Chu, W. Yan, X. Zhang, Ulk1/FUNDC1 prevents nerve cells from hypoxia-induced apoptosis by promoting cell autophagy, Neurochem. Res. 43 (8) (2018) 1539–1548.
[75] Y. Xiao, W. Chen, Z. Zhong, L. Ding, H. Bai, H. Chen, H. Zhang, Y. Gu, S. Lu, Electroacupuncture preconditioning attenuates myocardial ischemia-reperfusion injury by inhibiting mitophagy mediated by the mTORC1-ULK1-FUNDC1 pathway, Biomed. Pharmacother. 127 (2020) 110148.